Open access • Journal Article • DOI:10.1109/TGRS.1982.4307519

Crop Classification Using Airborne Radar and Landsat Data — Source link

Fawwaz T. Ulaby, Robert Y. Li, K. S. Shanmugan

Institutions: University of Kansas

Published on: 01 Jan 1982 - IEEE Transactions on Geoscience and Remote Sensing (IEEE)

Topics: Radar imaging, Radar and Scatterometer

AgRISTARS

SR-K1-04043
NAS 9-15421

A Joint Program for Agriculture and Resources Inventory Surveys Through Aerospace Remote Sensing

Supporting Research

February 1981

CROP CLASSIFICATION USING AIRBORNE RADAR AND LANDSAT DATA

F. T. Ulaby, R. Y. Li and K. S. Shanmugam

Remote Sensing Laboratory
University of Kansas Center for Research Inc.
2291 Irving Hill Drive - Campus West
Lawrence, Kansas 66045

Lyndon B. Johnson Space Center
Houston, Texas 77058

1. Report No.	2. Government Accession No.	3. Recipient's Catalog No.
RSL TR 360-13; SR-K1-04043		

4. Title and Subtitle	5. Report Date
Crop Classification Using Airborne Radar and Landsat Data	February 1981
	6. Performing Organization Code

7. Author(s)	8. Performing Organization Report No
F. T. Ulaby, R. Y. Li and K. S. Shanmugam	
	10. Work Unit No.

9. Performing Organization Name and Address	11. Contract or Grant No.
Remote Sensing Laboratory University of Kansas Center for Research, Inc. 2291 Irving Hill Drive - Campus West Lawrence, Kansas 66045	NAS 9-15421
	13. Type of Report and Period Covered
12. Sponsoring Agency Name and Address	Interim Report
NATIONAL AERONAUTICS AND SPACE ADMINISTRATION Lyndon B. Johnson Space Center Houston, Texas 77058	14. Sponsoring Agency Code

15. Supplementary Notes

16. Abstract

Airborne radar data acquired with a 13.3 GHz scatterometer over a test-site near Colby, Kansas were used to investigate the statistical properties of the scattering coefficient of three types of vegetation cover and of bare soil. A statistical model for radar data was developed that incorporates signal-fading and natural within-field variabilities. Estimates of the within-field and between-field coefficients of variation were obtained for each cover-type and compared with similar quantities derived from Landsat images of the same fields. The second phase of this study consisted of evaluating the classification accuracy provided by Landsat alone, radar alone, and both sensors combined. The results indicate that the addition of radar to Landsat improves the classification accuracy by about 10 percentage-points when the classification is performed on a pixel basis and by about 15 points when performed on a field-average basis.

17. Key Words (Suggested by Author(s))		18. Distribution Statement
remote sensing	Landsat	Unlimited
earth resources	radar	
agricultural crops		
crop classification		

19. Security Classif. (of this report)	20. Security Classif. (of this page)	21. No. of Pages	22. Price*
Unclassified	Unclassified	38	

*For sale by the National Technical Information Service, Springfield, Virginia 22161

THE UNIVERSITY OF KANSAS CENTER FOR RESEARCH, INC.

2291 Irving Hill Drive—Campus West
Lawrence, Kansas 66045

Telephone: (913) 864-4832

CROP CLASSIFICATION USING AIRBORNE RADAR AND LANDSAT DATA

Remote Sensing Laboratory
RSL Technical Report 360-13

F. T. Ulaby
R. Y. Li
K. S. Shanmugam

February 1981

Fawwaz T. Ulaby, Principal Investigator

Supported by:
NATIONAL AERONAUTICS AND SPACE ADMINISTRATION
Lyndon B. Johnson Space Center
Houston, Texas 77058
CONTRACT NAS 9-15421

TABLE OF CONTENTS

LIST OF FIGURES

LIST OF TABLES

CROP CLASSIFICATION USING AIRBORNE RADAR AND LANDSAT DATA

F. T. Ulaby, R. Y. Li and K. S. Shanmugam
Remote Sensing Laboratory
University of Kansas Center for Research, Inc.
Lawrence, Kansas 66045

ABSTRACT

Airborne radar data acquired with a 13.3 GHz scatterometer over a test-site near Colby, Kansas were used to investigate the statistical properties of the scattering coefficient of three types of vegetation cover and of bare soil. A statistical model for radar data was developed that incorporates signal-fading and natural within-field variabilities. Estimates of the within-field and between-field coefficients of variation were obtained for each cover-type and compared with similar quantities derived from Landsat images of the same fields. The second phase of this study consisted of evaluating the classification accuracy provided by Landsat alone, radar alone, and both sensors combined. The results indicate that the addition of radar to Landsat improves the classification accuracy by about 10 percentage-points when the classification is performed on a pixel basis and by about 15 points when performed on a field-average basis.

1.0 INTRODUCTION

Over the past several years, Landsat's Multispectral Scanners (MSS) have provided a continuous stream of multitemporal images for a large portion of the earth's surface. The availability of such a data-source has led to numerous investigations of the crop-classification capabilities and limitations of optical sensors. One of the major conclusions of these studies is that, in order to achieve high correct-classification rates, it is necessary to have uninterrupted (cloud-free) coverage of the area under investigation for successive passes. One way to rectify this interruption problem is to use radar, which effectively is immune to the presence of clouds in the atmosphere. If used in conjunction with optical sensors, radar can, potentially: (a) improve the crop-classification rates under clear-sky conditions because it responds to the geometrical and dielectric properties of vegetation [1-4] differently than do optical sensors, and (b) serve as a "substitute" for optical sensors during cloud-cover conditions.

Several crop-classification studies have been conducted using single- and/or two-date radar imagery [5-9], but no investigations have yet been reported in which periodic, repetitive coverage with imaging radar over the full growing-season has been employed. The first attempt to evaluate the significance of multitemporal radar observations was made by simulating radar imagery based on data acquired by a truck-mounted radar system [4] and by incorporating system parameters (resolution, signal-fading, etc.) and target parameters (slope, within- and between-field variance) in the simulation procedure. However, a simulated image is inherently limited by the assumptions and statistical distributions used in its generation. The above study was extended a step further by evaluating the combined Landsat/radar multitemporal crop classification wherein the radar data consisted of simulated images of the same scene observed by Landsat's MSS [10]. Again, the basic source of radar data was a truck-mounted radar. Similar studies also were conducted in Canada using single-date data acquired by airborne optical and radar scatterometer systems [11].

In 1978, seven missions were flown by NASA/Johnson Space Center's C-130 aircraft over an agricultural test-site near Colby, Kansas in support of a soil-moisture investigation. Among the host of sensors used was a 13.3 GHz radar scatterometer (non-imaging). To date, the data acquired in the first two flights have been processed by NASA/JSC and made available for analysis. These data are used in the present study to: (a) investigate the statistical nature of the radar backscattering coefficient for bare ground and for three different crop-types, including within-field and between-field variations, and (b) evaluate the crop-classification rates obtained using Landsat alone, radar alone, and both combined.

2.0 EXPERIMENT DESCRIPTION

The test site used for this investigation is located near Colby, Kansas, in the northwestern part of the state. The available radar-data consist of backscatter measurements for seven flight-lines, acquired by the NASA/JSC 13.3 GHz scatterometer from an altitude of 460 m above the ground. The scatterometer is a fan-beam Doppler system, VV polarized, and has a 2.5° beamwidth in the cross-track direction. The Doppler spectrum was processed to yield a 37-m resolution in the along-track direction. Although the scatterometer was used to measure the backscattering coefficient at several angles of incidence (relative to nadir) between 5° and 60°, only the 50° data are used in this study in order to minimize the effects of soil moisture variations on crop identification. For $\theta = 50°$, the resolution-cell size is 37 m x 31 m. As the aircraft bearing the scatterometer flew across, the scatterometer measured the return from 10 contiguous cells within each field, with the field-size being approximately 400 m x 400 m. In this study, the analysis is based on data for 36 fields (Table 1), for which detailed ground-truth information is available and which appear spatially "homogeneous" on aerial photography. Ground observations include crop-type and height, row spacing, soil moisture content and vegetation moisture content (for a limited number of fields).

Because of the coherent nature of the transmitted signal, the backscattered energy measured by a radar system exhibits random

TABLE 1

Distribution of Fields Among Cover Categories

Cover	Number of Fields (Each 400 m x 400 m)
Wheat Stubble	12
Corn	11
Fallow (Bare Soil)	10
Pasture (Short Grass)	3

fluctuating component of the received signal, spatial and/or frequency averaging usually is used. For a given set of radar and flight parameters, the number of independent samples, N, incorporated in the measurement of the power backscattered from a given ground cell is determined easily through readily available expressions; in the case of the Doppler scatterometer used for this investigation, N = 69 for each 37 m x 31 m cell [12]. Assuming Rayleigh statistics [13], the received power is described by a Chi-square distribution with 2N degrees of freedom, whose mean, S, (for a given cell) is related to the variance σ^2 of the distribution through

$$\frac{\sigma^2}{S^2} = \frac{1}{N} \qquad (1)$$

For N larger than about 20, the Chi-square distribution approaches a truncated normal distribution, which is a valid approximation in the present case (N = 69). This information will be used in the next section for evaluating the within-field variance due to differences in the scattering properties of different cells within the same field (over and above the variance due to fading).

3.0 STATISTICAL PROPERTIES

The next section is concerned with the application of classification techniques using the available radar data and Landsat MSS data for the same fields. The Landsat images were recorded on 26 July 1978, approximately a week after the July 18 and 20, 1978, radar flights. The statistical properties of the radar and optical data are discussed in this section, as a precursor to the classification task (next section).

3.1 Definitions and Notations

The 36 available fields are distributed among four categories: wheat stubble, corn, fallow (bare ground), and pasture (grass), with an approximately even distribution among the first three (Table 1) and only three fields of pasture. For each cat

I_{ij} = Landsat image tonal value (for a given band) of the j^{th} pixel of the i^{th} field

S_{ij} = measured radar scattering coefficient of the j^{th} pixel of the i^{th} field

N_f = number of fields (for the category under consideration)

$N_{c\ell}$ = number of Landsat cells (pixels) per field = 30

N_{cr} = number of radar cells per field = 10

N = number of independent samples incorporated in the measurement of S_{ij}; $N = 69$ in this case

$\mu_{i\ell}$ = mean Landsat image value for field $i = E_j(I_{ij})$

$$\hat{\mu}_{i\ell} = \frac{1}{N_{c\ell}} \sum_{j=1}^{N_{c\ell}} I_{ij} \qquad (2)$$

μ_{ir} = mean radar scattering coefficient values for field $i = E_j(S_{ij})$

$$\hat{\mu}_{ir} = \frac{1}{N_{cr}} \sum_{j=1}^{N_{cr}} S_{ij} \qquad (3)$$

$$\mu_{\ell} = E_i(\mu_{i\ell}) \qquad (4)$$

$$\mu_r = E_i(\mu_{ir}) \qquad (5)$$

Equations (4) and (5): Population means for all cells of all fields of the category under consideration

3.2 Between-Field Variance

The between-field variance for a given category is given by:

$$\sigma^2_{BF\ell} = E_i(\mu^2_{i\ell}) - \mu^2_\ell \quad \text{, for Landsat} \tag{5}$$

and

$$\sigma^2_{BFr} = E_i(\mu^2_{ir}) - \mu^2_r \quad \text{, for radar} \tag{7}$$

Table 2 shows estimated values of the coefficients of variation, $\hat{C}_{BF\ell} = \hat{\sigma}_{BF\ell}/\hat{\mu}_\ell$ for Landsat and $\hat{C}_{BFr} = \hat{\sigma}_{BFr}/\hat{\mu}_r$ for radar, for each of the four categories. These results indicate that the coefficient of variation for between-field variations is several times larger for radar than for Landsat. Part of the variability in the radar data is attributed to system measurement precision. However, on the basis of radar measurements from individual "homogeneous" targets, the system variability is estimated to contribute less than 30 percent to the values given in Table 2.

3.3 Within-Field Variance

A. Landsat

In the Landsat image, variations in intensity among pixels of a given field are due to natural variations between different parts of the field, even though the field may be characterized as nomogeneous on the basis of ground-truth information. The within-field variance for a field i is given by

$$\sigma^2_{wi\ell} = E_j(I^2_{ij}) - \mu^2_{i\ell} \tag{8}$$

and the coefficient of variation for field i

$$C_{wi\ell} = \sigma_{wi}/\mu_{i\ell} \tag{9}$$

TABLE 2

Average Within-Field and Between-Field
Coefficients of Variation

	Within-Field: $\left(\frac{\overline{\hat{\sigma}_{wi}}}{\hat{\mu}_i}\right)$		Between-Field: $\left(\frac{\hat{\sigma}_{BF}}{\hat{\mu}}\right)$	
Category	Radar	Landsat (Band 4)	Radar	Landsat (Band 4)
Wheat Stubble	0.21	0.08	0.26	0.10
Corn	0.16	0.10	0.35	0.05
Fallow	0.17	0.07	0.25	0.05
Pasture	0.13	0.06	0.30	0.05

Estimated values of $C_{w\ell}$ are given in Table 2 for each of the four categories.

B. Radar

Computation of the within-field variability due to natural variations within a given field is not as straightforward for the radar data as it is for the Landsat image. The reason is signal-fading due to the partially coherent nature of the radar measurements. Thus, the variability within a field is attributed to two statistical processes: natural variability and fading variability. The latter is governed by the radar measurement technique and therefore it is system-dependent. If the radar measurement were made with an incoherent system or, equivalently, if the measurement is an average of a very large number of independent samples, then the only variability that would be observed among different cells of the same field would be due to natural variability. The purpose of this section is to determine the within-field variance for such an incoherent system, and to develop a model for radar data that can be applied to any coherent radar system whereby the two sources of variance may be incorporated.

The scattering coefficient S_{ij} of the j^{th} cell of the i^{th} field may be modeled by a multiplicative model [13,14] of the form:

$$S_{ij} = \mu_i \cdot Y_{ij} \cdot Z_N \qquad (11)$$

where

μ_i = true mean scattering coefficient of field i,

Y_{ij} = random variable accounting for the within-field natural spatial variability, $E_j(Y_{ij}) = \mu_{Y_i} = 1$ for all i,

Z_N = random variable accounting for signal fading, Z_N is described by a normalized x^2 distribution with 2N degrees of freedom, $E(Z_N) = 1$.

For $N > 20$, the x^2 distribution approaches a truncated normal distribution and Z_N may be described by

$$Z_N = 1 + \left(\frac{X}{\sqrt{N}}\right) \quad ; \qquad Z_N \geq 0 \qquad (12)$$

where X is a zero-mean random variable described by a truncated normal distribution such that $Z_N \geq 0$.

To compute the variance of Y_{ij} for a given field i, we first convert (11) into an additive model by expressing the terms in decibels (dB),

$$10 \log S_{ij} = 10 \log \mu_i + 10 \log Y_{ij} + 10 \log Z_N \qquad (13)$$

or

$$S'_{ij} = \mu'_i + Y'_{ij} + Z'_N \qquad (14)$$

where $S'_{ij} \triangleq 10 \log S_{ij}$, and similarly for the other terms. The random variables Y_{ij} and Z_N, accounting respectively for the natural spatial variability and for the fading variability, are governed by independent physical processes, and therefore they may be considered statistically independent. With μ'_i(dB) being a constant for field i, the variance of S'_{ij}(dB) is

$$\sigma^2_{S'_i} = \sigma^2_{Y'_i} + \sigma^2_{Z'_N} \qquad (15)$$

The variance $\sigma^2_{S'_i}$ is computed from measured values of S'_{ij} for $j = 1, N_{cr}$. To compute the variance $\sigma^2_{Z'_N}$, we first need to determine the probability density function $f_{Z'_N}(Z'_N)$. The random variable Z'_N is given by

$$\begin{aligned} Z'_N &= 10 \log \left(1 + \frac{X}{\sqrt{N}}\right) \\ &= 10 \log (\sqrt{N} + X) - 10 \log \sqrt{N} \qquad (16) \\ &= T + 10 \log \sqrt{N} \end{aligned}$$

where $T \triangleq 10 \log (\sqrt{N} + X)$ (17)

As was stated earlier, X is described by a truncated zero-mean normal distribution,

$$f_X(X) = \frac{1}{\sqrt{2\pi}} \exp\left(-\frac{X^2}{2}\right) \qquad -\sqrt{N} \leq X \leq \infty \qquad (18)$$

with the lower limit being mandated by the fact that Z_N cannot be negative because it represents power.

From (17) and (18) the probability density function of T is given by:

$$f_T(T) = J\, f_X(X)$$

where J is the Jacobian,

$$J = \frac{dX}{dT} = 10^{T/10} \ln 10$$

Hence,

$$f_T(T) = \frac{\ln 10}{\sqrt{2\pi}}\ 10^{T/10}\ \exp\left[-\frac{(10^{T/10} - \sqrt{N})^2}{2}\right] \quad , -\infty \le T \le \infty \qquad (19)$$

Finally, using (16), a change of variables leads to

$$f_{Z'_N}(Z'_N) = \frac{\ln 10}{\sqrt{2\pi}}\ 10^{Z''_N}\ \exp\left[-\frac{(10^{Z''_N} - \log\sqrt{N})^2}{2}\right] \quad , -\infty \le Z'_N \le \infty \qquad (20)$$

where

$$Z''_N \triangleq \frac{Z'_N}{10} - \log\sqrt{N} \qquad (21)$$

Plots of $f_{Z'_N}(Z'_N)$ are shown in Figure 1 for N = 16 and N = 64; the curves are skewed-normal in shape.

Using (20), the variance $\sigma^2_{Z'_N}$ was computed for several values of N and is shown in Figure 2.

For the radar scatterometer data available to this study, N = 69 [12] on the basis of the sensor and aircraft parameters and the usually assumed Rayleigh fading model. With N known, $\sigma^2_{Z'_N}$ was computed empirically using the density function given in (20) and then used in (15) to determine σ_{Y_i}, the within-field variance due to natural spatial variability (σ_{S_i} was estimated from measured values of S'_{ij}, as stated earlier). After repeating this process for all fields of each category, the average values of σ_{S_i} and σ_{Y_i} over i were computed and are given in Table 3.

For comparison to Landsat, the variance σ^2_Y is obtained from $\sigma^2_{Y'}$, by assuming that Y' is normally distributed. This assumption is based on the observation that the scattering coefficient of vegetation targets is approximately normally distributed when expressed in dB [15]. Further, 33 out of 36 fields passed the Kolmogorov-Smirnov normality test [17]

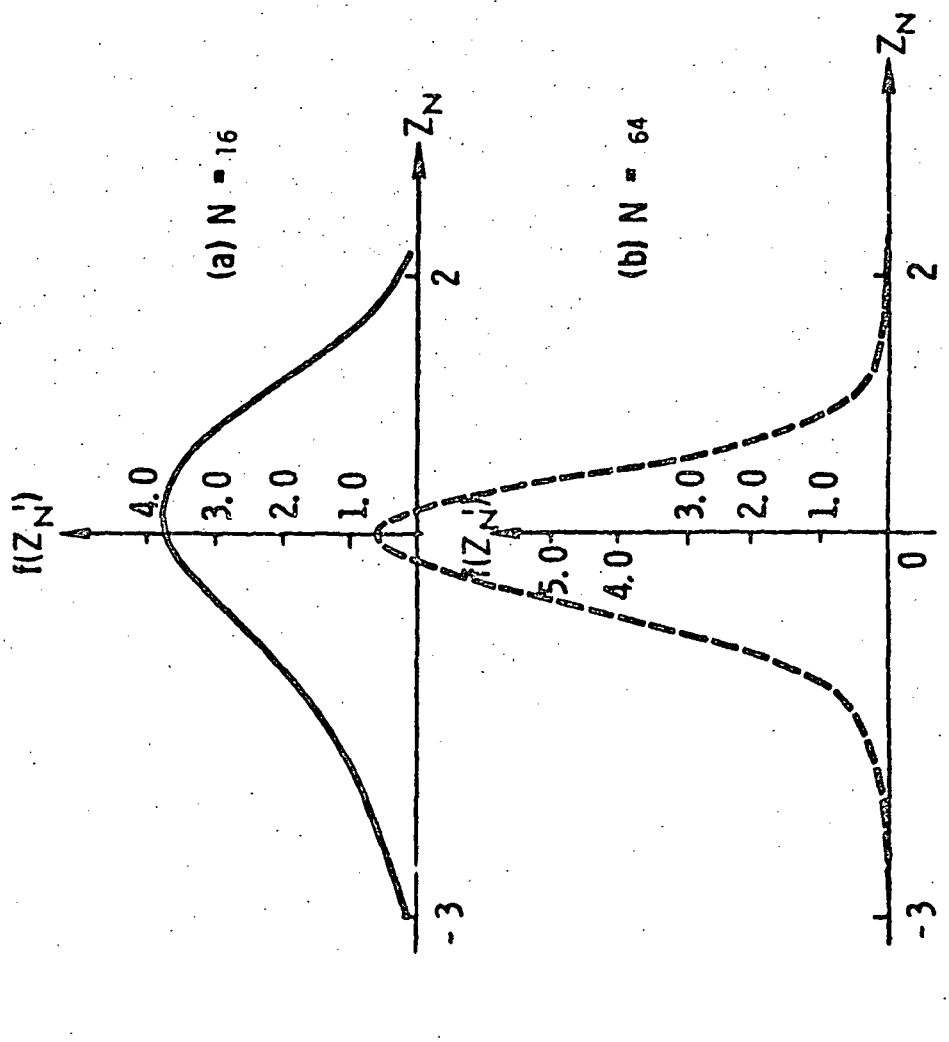

Figure 1. Plots of the probability density function $f(Z_N')$ for (a) N = 16, and (b) N = 64.

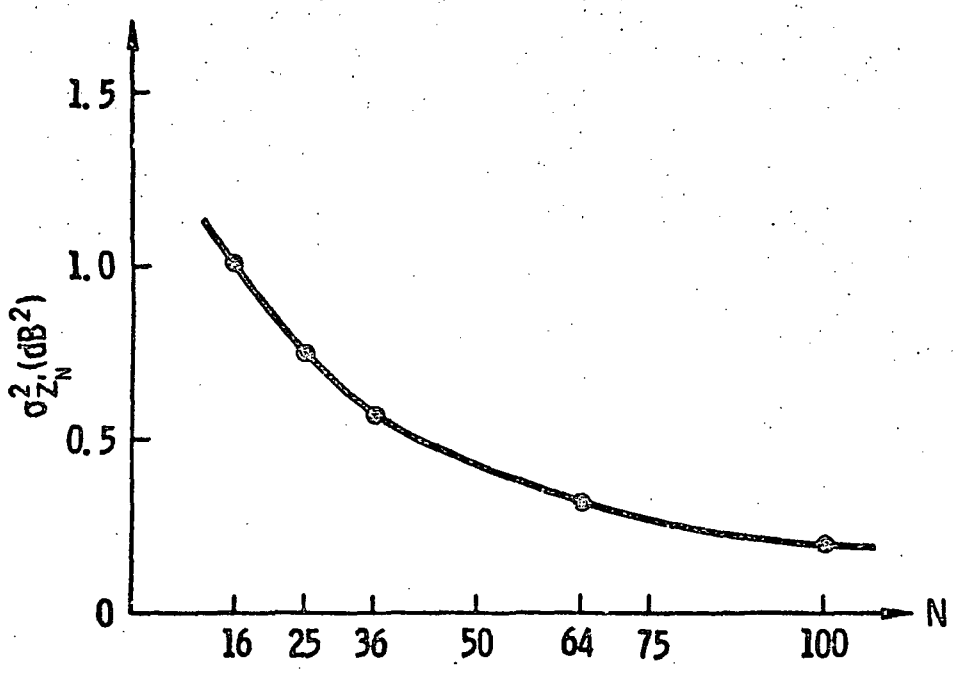

Figure 2. Plot of $\sigma^2_{Z_N}$ as a function of the number of the independent samples N.

TABLE 3

Relative Contributions of Fading (with N = 69) and Spatial Variances to the Total Within-Field Variance of S' (Scattering Coefficient in dB)

	Average Total Within-Field Variance, $\hat{\sigma}^2_S$,	Relative Contributions	
		Fading, $\hat{\sigma}^2_Z$,	Spatial Variation, $\hat{\sigma}^2_Y$,
Wheat Stubble	1.10 dB^2	0.28 dB^2	0.82 dB^2
Corn	0.76 dB^2	0.28 dB^2	0.48 dB^2
Fallow	0.83 dB^2	0.28 dB^2	0.55 dB^2
Pasture	0.94 dB^2	0.28 dB^2	0.66 dB^2

at the 0.05 significance-level when applied to S'_{ij} (scattering coefficient expressed in dB). From

$$Y'_{ij} = 10 \log Y_{ij} = 4.3 \ln Y_{ij} \quad (22)$$

we define

$$Y''_{ij} = \frac{Y'_{ij}}{4.3} = \ln Y_{ij} \quad (23)$$

For a given field i, Y'_{ij} (and therefore Y''_{ij}) is assumed to be normally distributed. Hence, the variance of Y_i is given by [18]:

$$\sigma^2_{Y_i} = \mu_{Y_i} [\exp(\sigma^2_{Y''_i}) - 1] = \exp(\sigma^2_{Y''_i}) - 1 \quad (24)$$

since $\mu_{Y_i} = 1$ for all i. Converting back to Y'_i, we have

$$\sigma^2_{Y_i} = \exp\left(\frac{\sigma^2_{Y'_i}}{18.5}\right) - 1 \quad (25)$$

Using the values of $\sigma^2_{Y'_i}$ computed earlier, $\sigma^2_{Y_i}$ was obtained for each value of i using the above expression. The average value of Y_i over i is given in Table 2 for the four cover categories. The results given in Table 2 indicate that radar data exhibit much larger within-field variability compared to Landsat data.

For each category, the total variance σ^2_T is computed from:

$$\sigma^2_T = E_{ij}[(S'_{ij})^2] - (\mu')^2 \quad (26)$$

where the averaging is performed over all S'_{ij} values, with $j = 1, N_{cr}$ and $i = 1, N_f$, and $\mu' = 10 \log \mu_r$. Thus, σ^2_T includes all sources of variance including fading, within-field and between-field. Table 4 compares the values of σ_T computed from the 1978 data with the results

TABLE 4

Comparison of Total Standard Deviation $\hat{\sigma}_T$, Incorporating Fading, Within-Field and Between-Field Variations

		Wheat	Corn	Bare Soil	Milo
$\hat{\sigma}_T$, dB	6/26/70	1.05	1.3	1.35	1.65

		Wheat Stubble	Corn	Bare Soil	Pasture
$\hat{\sigma}_T$, dB	7/18/78	1.37	1.6	1.39	1.59

1970: 13.3 GHz VV, 600 measurements [16]

1978: 13.3 GHz VV, 360 measurements [this study]

from a similar data set obtained in 1970 [16] with the same radar scatterometer system. It is noted that the two sets of values are comparable in magnitude and range, although not all the categories are identical for the two data sets. Histograms of S'_{ij} are shown in Figures 3-5 for corn, wheat stubble, and bare soil. The histograms appear approximately normal in shape.

4.0 CLASSIFICATION RESULTS

The available radar data were obtained from flights on 7/18/78 and 7/20/78. Usually, one would not expect any significant additional information to be derived from the second flight, since it was in such close time-proximity to the first one except, in this case, a rainfall of 1.9 cm occurred on 7/19/78, the day between the two flights. Hence, this occasion provides an opportunity to evaluate the effect of rain on crop-identification accuracy.

The cloud-free Landsat pass in closest proximity to the radar flights was on 7/26/78, approximately a week after the radar acquisition dates. In the discussion below, the classification results obtained on the basis of the Landsat data above will be presented first, followed by presentations of the radar results and the results obtained using both types of sensors in combination.

4.1 Landsat Alone

A total of 1,080 Landsat pixels were available for classification. Using a linear Bayes classifier, the results shown in Figure 6 were obtained. On a single-band basis, Band 4 gave the best results with 67% of the pixels being correctly recognized. The addition of the other bands improved the classification accuracy to 75%. The crop confusion table for Band 4 alone is given in the top part of Table 5.

4.2 Radar Alone

The distributions of values for the field-mean scattering coefficient are shown in Figure 7 for each cover category. Indicated on each vertical bar are the maximum, mean, and minimum values of μ'_{ir}.

Figure 3. Histogram of S'(dB) for wheat stubble on 7/18/78.

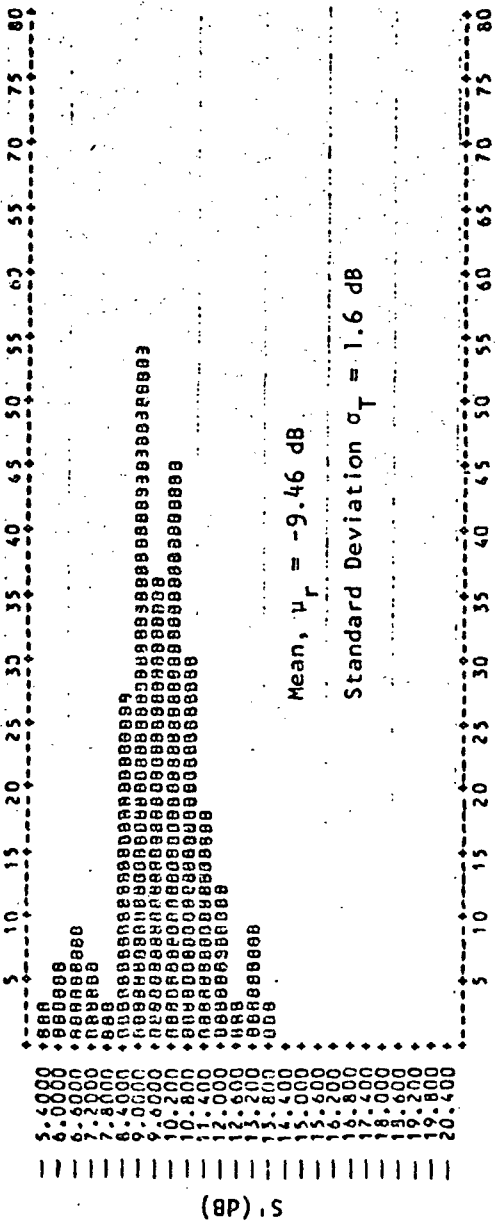

Figure 4. Histogram of S'(dB) for corn on 7/18/78

^ denotes estimated values

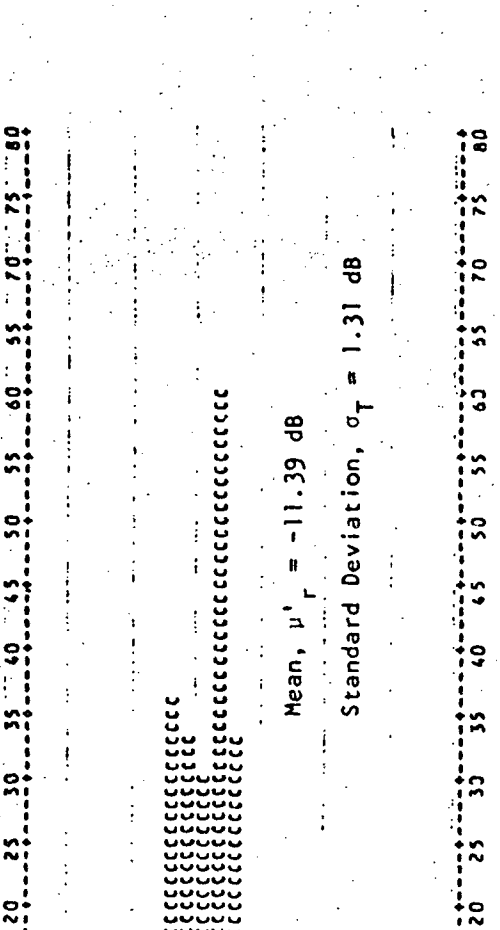

Figure 5. Histogram of S'(dB) for bare soil on 7/18/78.

coefficient of variation is:

$$C_{w\ell} = E_i(C_{wi\ell}) \qquad (10)$$

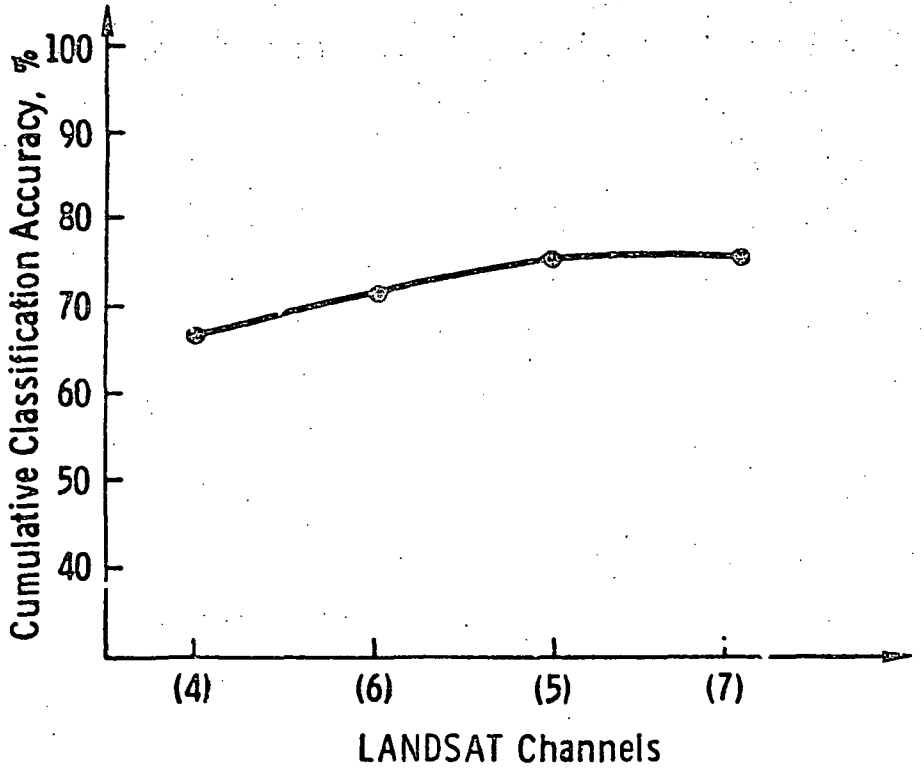

Data Form: LANDSAT Bands 4, 5, 6 and 7
Pixels Used: 1080
Categories: Wheat Stubble, Corn, Fallow and Pasture
Date: July 26, 1978

TABLE 5

Crop Confusion Tables for (a) Landsat Alone, (b) Radar Alone, and (c) Both Combined

(a) Landsat Alone

Classified as → / Actual	Wheat Stubble	Corn	Fallow	Pasture
Wheat Stubble	29.2	1.0	30.3	39.4
Corn	0.6	93.7	0.0	5.8
Fallow	9.0	0.7	88.3	2.0
Pasture	36.7	0.0	13.3	50.0

Feature Used: Landsat Imagery Band 4 on 7/26/78

Total Classification Accuracy: 67.0%

(b) Radar Alone

Classified as → / Actual	Wheat Stubble	Corn	Fallow	Pasture
Wheat Stubble	70.8	1.6	8.3	19.1
Corn	3.6	70.0	26.3	0.0
Fallow	13.0	19.0	68.0	0.0
Pasture	13.3	0.0	0.0	86.6

Feature Used: Radar Measured Pixels (dB) on 7/18/78

Total Classification Accuracy: 71.1%

TABLE 5 (contd.)

(c) Landsat and Radar

Actual \ Classified as →	Wheat Stubble	Corn	Fallow	Pasture
Wheat Stubble	71.3	1.6	7.7	19.1
Corn	2.1	95.7	2.1	0.0
Fallow	7.0	1.0	92.0	0.0
Pasture	13.3	0.0	0.0	86.6

Feature Used: Landsat Band 4 on 7/26/78 and Radar Measured Pixels (dB) on 7/18/78

Total Classification Accuracy: 85.8%

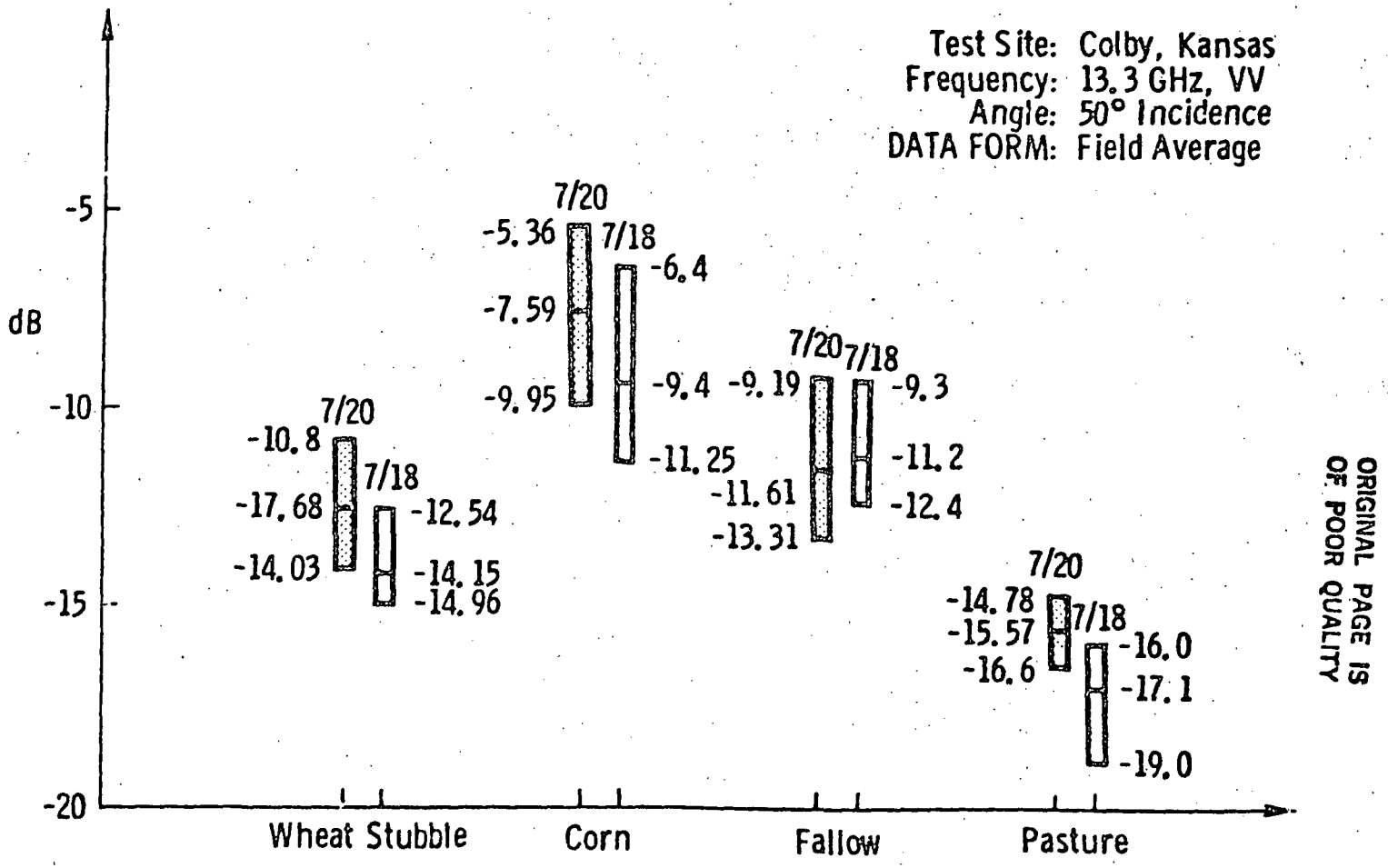

Figure 7. Distributions of field averages of agricultural fields for both July 18 (before rain) and July 20 (after rain) radar data. Upper and lower bounds are maximum and minimum values of μ'_{ir} and the in-between level is the average value.

day varied the range of values of μ'_{ir} for all categories except bare soil (fallow). For the entire data set as a whole, its mean value is 1.0 dB higher for the 7/20/78 flight than for the 7/18/78 flight. On a relative basis, the main effect of the rain is the greater overlap of the range of values of wheat stubble and fallow, which is likely to result in increased confusion between these two categories.

Single-date and multi-date radar classification results are shown in Figure 8, and the crop confusion tables are given in Table 6 for each of the two dates. The poorer results for the 7/20/78 flight are due to increased confusion between wheat stubble and fallow, as expected.

Figure 9 compares the correct classification rates obtained on a pixel-by-pixel basis with those obtained on a field-by-field basis and, where for the former the radar classification was performed on S'_{ij}, for the latter it was performed on S'_i, the average scattering coefficient of field i ($S'_i = 10 \log S_i = 10 \log \sum_{j=1}^{N_{cr}} S_{ij}$). Substantial improvement in classification accuracy is observed for the radar if field averages rather than pixel values are used in the classification, due to larger within-field variance in radar data. The improvement is much smaller for Landsat.

4.3 Landsat-Radar Combined

Following a procedure in which the radar resolution cells were stretched and skewed to match the Landsat pixels for each field, a matched set of Landsat-radar values were generated. Figures 10a and 10b show the cumulative classification accuracy obtained using the Landsat image of 7/26/78, combined with the radar data of 7/18/78 and 7/20/78, respectively. In both cases the Landsat Band 4 was chosen as the best first feature (highest F-ratio) followed by the radar. Combination of the 7/18/78 radar data and the Landsat data yields a performance of 85%, in comparison to 75% for Landsat alone. The improvement is smaller when Landsat data is combined with the 7/20/78 radar data. When all four Landsat bands and both radar dates are used, the maximum correct classification accuracy obtained is 89.4%. The crop confusion tables for Landsat alone, radar (7/18/78) alone, and the combination of the two, are given in Table 5.

Cumulative classification results on a field-by-field basis, and the associated confusion table, are given in Figure 11.

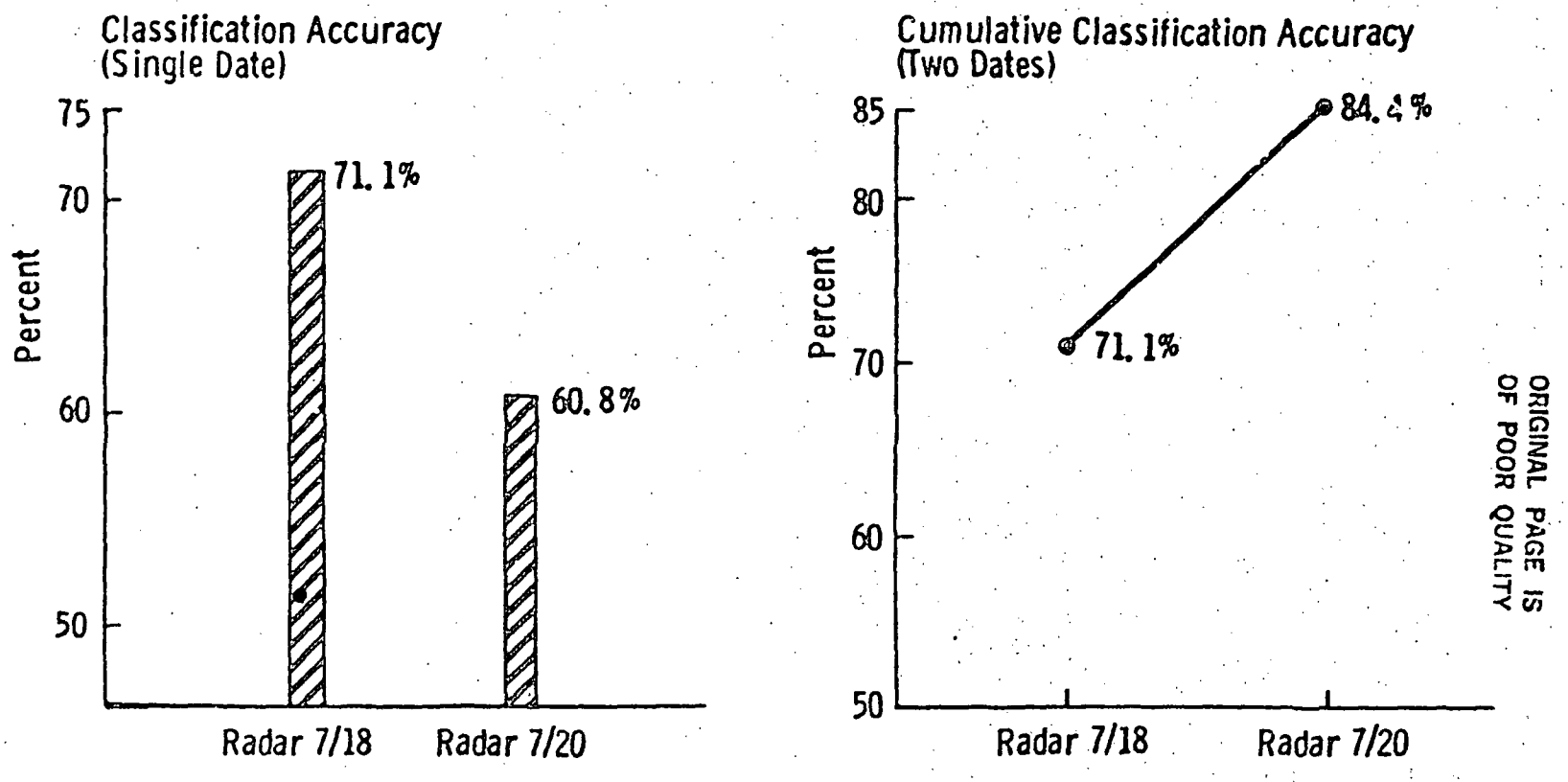

Figure 8. Radar classification performance using measured pixels, S'(dB), for the 7/18/78 and 7/20/78 flights.

TABLE 6

Crop Confusion Tables for Radar Flights
of 7/18/78 and 7/20/78
(Before and After Rain)

7/18/78 Flight:
(Before Rain)

7/18/78	% Classified			
	Wheat Stubble	Corn	Fallow	Pasture
Wheat Stubble	70.8	1.6	8.3	19.1
Corn	3.6	70.0	26.3	0.0
Fallow	13.0	19.0	68.0	0.0
Pasture	13.3	0.0	0.0	86.6

Total Classification Accuracy = 71.1%

7/20/78 Flight:
(After Rain)

7/20/78	% Classified			
	Wheat Stubble	Corn	Fallow	Pasture
Wheat Stubble	39.1	0.0	34.1	26.6
Corn	0.0	91.8	8.1	0.0
Fallow	33.0	16.0	42.0	9.0
Pasture	3.3	0.0	0.0	96.6

Total Classification Accuracy = 60.8%
Data From: Measured Pixels S'_{ij}(dB)

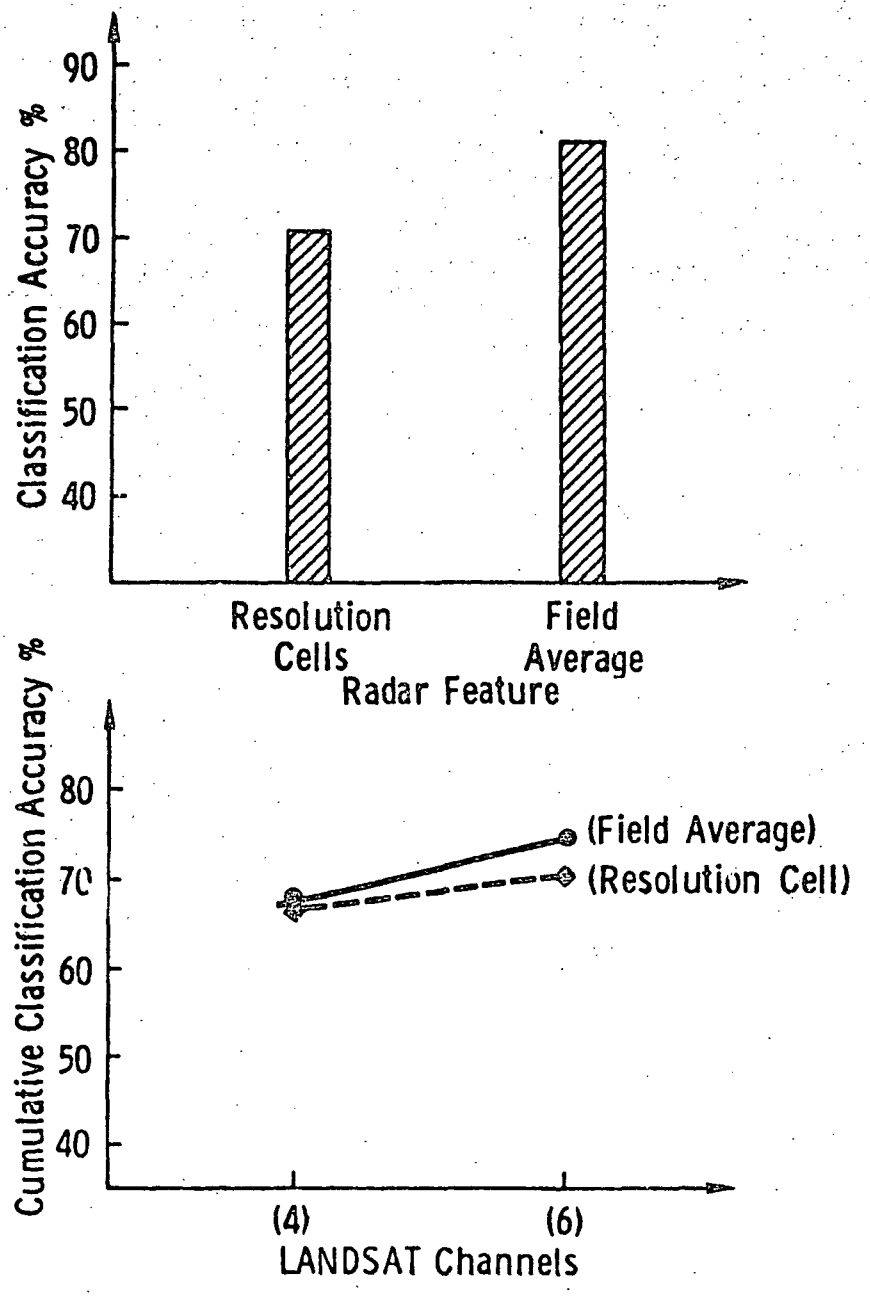

Figure 9. Comparison of classification accuracies obtained for classification applied on a pixel (cell) basis and on a field-average basis

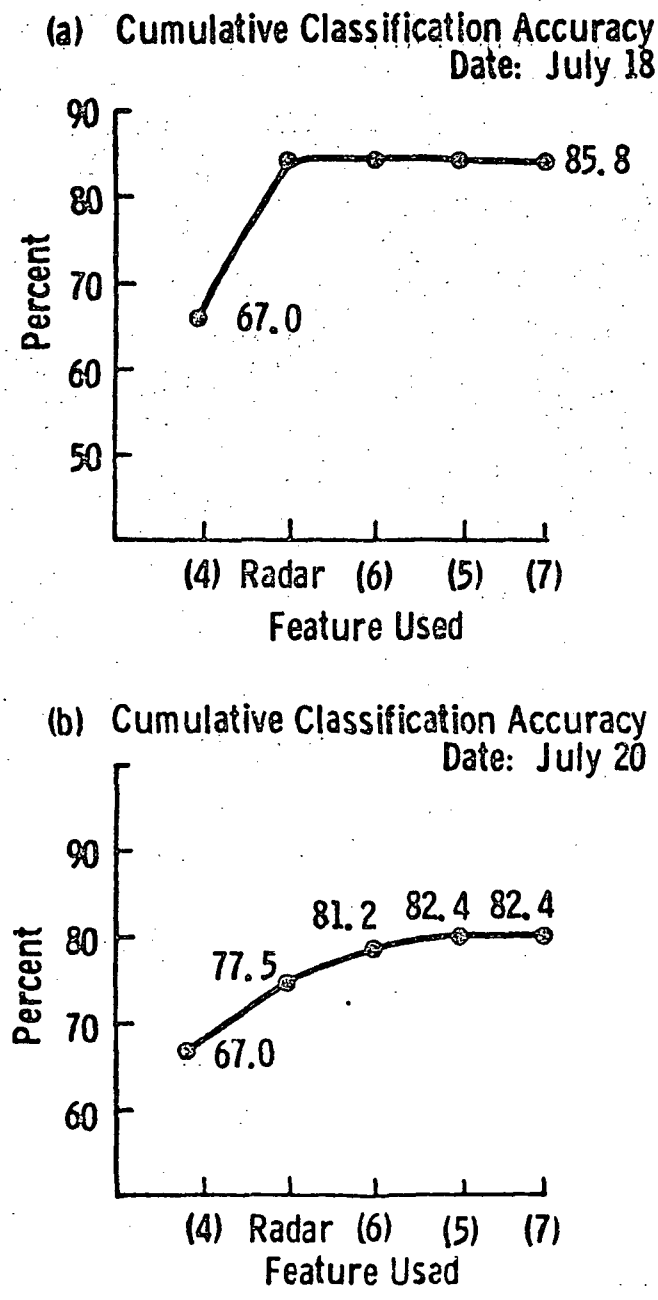

RADAR DATA FORM: Measured Pixels on 7/18/78 and 7/20/78. S'(dB)
LANDSAT DATA: Bands 4, 5, 6 & 7 on 7/26/78

Figure 10. Combined Landsat/radar classification

Combined Radar/Landsat Classification

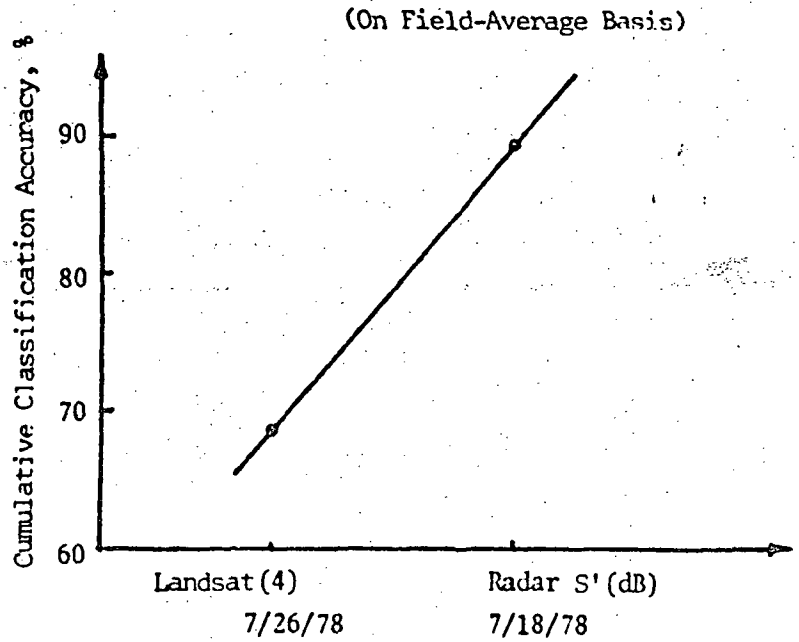

Crop Confusion Table

Actual \ Classified as →	Wheat Stubble	Corn	Fallow	Pasture
Wheat Stubble	9	0	2	1
Corn	0	11	0	0
Fallow	0	0	10	0
Pasture	0	0	0	3

4.4 Comparison of Classifiers

Throughout the preceding sections, the classification tests were performed using the linear Bayes classifier. For comparison purposes, tests were performed using the four different classifiers indicated in Figure 12. The Euclidean-distance classifier provides the poorest performance, while the quadratic Bayes classifier gives the highest classification accuracy. The minimum-square-error (MSE) and linear Bayes classifiers are comparable to each other in performance and are slightly inferior to the quadratic Bayes classifier.

5.0 CONCLUSIONS

The major contributions and conclusions of this study are:

(a) A statistical model for radar backscatter was developed that accounts for the winthin-field natural variability and for signal-fading, simultaneously. The model was applied to derive estimates of the within-field coefficient of variation and the results were compared with the same quantity derived from Landsat image data.

(b) Estimates for the Landsat and radar between-field coefficients of variation were copmuted and compared. The results show that the radar data exhibit larger within-field and between-field variations.

(c) Adding radar to Landsat improves the correct classification accuracy by about 10 percentage-points when classification is performed on a pixel basis and by about 15 percentage-points on a field basis. Of course, in the absence of Landsat coverage due to clouds, the radar becomes the prime sensor for monitoring crops.

(d) The results obtained in this study pertain to the cover-types, geographic location and time-period specified. Further research is needed to evaluate the statistical nature of the radar backscatter and the combined performance of optical and radar sensors using multi-date data and other geographic regions.

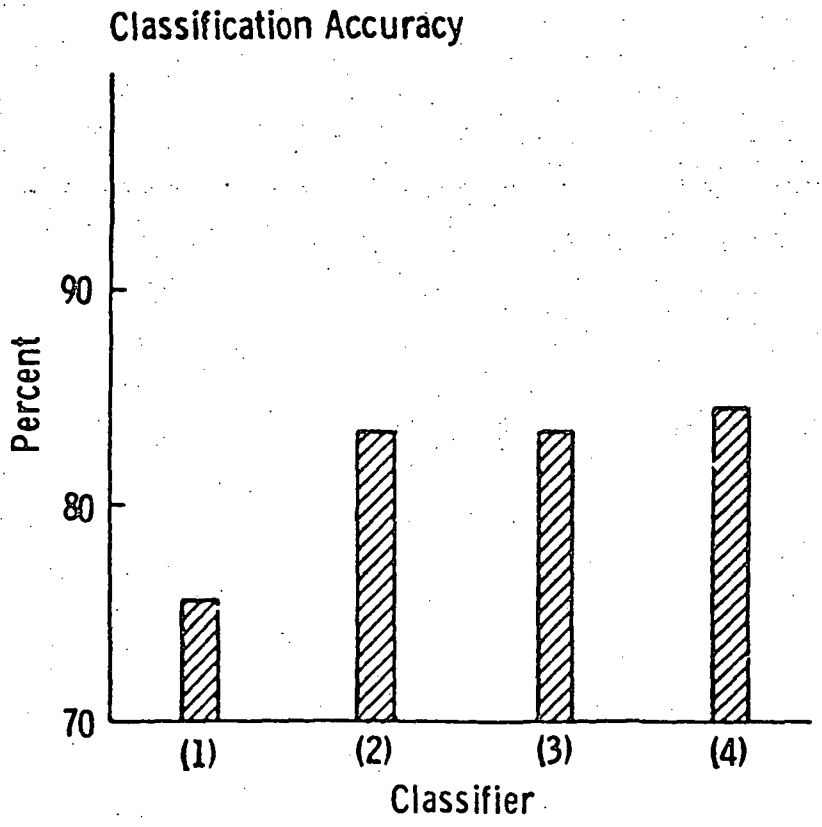

(1) Euclidean- Distance
(2) MSE
(3) Linear Bayes
(4) Quadratic Bayes

Feature: LANDSAT (4) + Radar 13.3 GHz, VV
Pixels used: 1080

ACKNOWLEDGMENT

This research was supported by the National Aeronautics and Space Administration, Lyndon B. Johnson Space Center, Houston, Texas, Contract NAS 9-15421.

REFERENCES

[1] Ulaby, F. T., "Radar Response to Vegetation," IEEE Trans. on Antennas and Prop., AP-23, No. 2, January 1975.

[2] Ulaby, F. T., G. A. Bradley and M. C. Dobson, "Microwave Backscatter Dependence on Surface Roughness, Soil Moisture and Soil Texture, Part II: Vegetation-Covered Soil," IEEE Trans. on Geoscience Electronics, GE-17, No. 2, pp. 33-40, April 1979.

[3] Ulaby, F. T., T. F. Bush and P. P. Batlivala, "Radar Response to Vegetation, II: 8-18 GHz Band," IEEE Trans. on Antennas and Prop., AP-23, No. 5, pp. 608-618, September 1975.

[4] Bush, T. F. and F. T. Ulaby, "An Evaluation of Radar as a Crop Classifier," Remote Sensing of Environment, 7, pp. 15-36, 1978.

[5] Simonett, D. S., J. E. Eagleman, A. B. Erhard, D. C. Rhodes and D. E. Schwarz, "The Potential of Radar as a Remote Sensor in Agriculture, I: A Study with K-Band Imagery in Western Kansas," CRES Report 61-21, University of Kansas, Lawrence, Kansas, 1967.

[6] Haralick, R. M., F. R. Caspall and D. S. Simonett, "Using Radar Imagery for Crop Discrimination: A Statistical and Conditional Probability Study," Remote Sensing of Environment, 1, pp. 131-142, 1972.

[7] Schwarz, D. E. and F. R. Caspall, "The Use of Radar in the Discrimination of Agricultural Land Use," in Proc. 5th Symp. Rem. Sens. of Env., 1, pp. 233-247, 1968.

[8] Ulaby, F. T., P. P. Batlivala and J. E. Bare, "Crop Identification with L-Band Radar," Photogrammetric Engineering and Remote Sensing, 46, No. 1, pp. 101-105, January 1980.

[9] Brisco, B. and R. Protz, "Corn Field Identification Accuracy Using Airborne Radar Imagery," Canadian J. Rem. Sens., 6, No. 1, July 1980, pp. 15-25.

[10] Li, R. Y., F. T. Ulaby and J. R. Eyton, "Crop Classification with a Landsat-Radar Sensor Combination," Proc. Symp. on Machine Processing of Remotely Sensed Data, Purdue University, West Lafayette, Indiana, June 2-6, 1980.

[11] Ahern, F. J., D. G. Goodenough, A. L. Grey, R. A. Ryerson and R. J. Vilbikaitis, "Simultaneous Microwave and Optical

[12] Bradley, G. A. and F. T. Ulaby, "Aircraft Radar Response to Soil Moisture," RSL Technical Report 460-2 (AgRISTARS Report SM-KO-04005), University of Kansas Center for Research, Inc., October 1980.

[13] Bush, T. F. and F. T. Ulaby, "Fading Characteristics of Panchromatic Radar Backscatter from Selected Agricultural Targets," IEEE Trans. Geoscience Electronics, GE-13, October 1976, pp. 149-157.

[14] Frost, V. C., J. A. Stiles, K. S. Shanmugam and J. C. Holtzman, "A System Model for Imaging Radars," Proc. 5th Int'l. Conf. on Pattern Recognition and Image Processing, Miami, Florida, December 1980.

[15] Ulaby, F. T., "Vegetation Clutter Model," IEEE Trans. on Antennas and Prop., AP-28, No. 4, July 1980, pp. 538-545.

[16] King, C., "Agricultural Terrain Scatterometer Observations with Emphasis on Soil Moisture Variation," RSL Technical Report 177-44, University of Kansas, Lawrence, Kansas, August 1973.

[17] Bradley, J. V., Distribution-Free Statistical Tests, Prentice-Hall, Englewood Cliffs, New Jersey, 1968.

[18] Panter, P. F., Communication System Design, McGraw-Hill, pp. 33-37, 1972.